

A spectral Conjugate Gradient method for solving unconstrained optimization problems

Mariya Toofan^{1,2*}, Gohar Shakouri³

The conjugate gradient (CG) method stands out as one of the most rapidly growing and effective approaches for addressing unconstrained optimization problems. In recent years, significant efforts have been dedicated to adapting the CG for tackling nonlinear optimization challenges. This research article introduces a new modification of the Fletcher–Reeves (FR) conjugate gradient method. The proposed method is characterized by its sufficient descent property, and its global convergence has been established under specific assumptions. Numerical experiments conducted on 96 functions from the CUTER collection demonstrate the potential and effectiveness of the proposed methods. The computational results show that the proposed MFR method achieves better performance in terms of function and gradient evaluations as well as CPU time compared to DPRP and FR, while remaining competitive with NRP. These findings confirm that enforcing the sufficient descent condition in equality form can provide both theoretical robustness and practical efficiency.

Keywords: Nonlinear optimization; line search; spectral conjugate gradient method; sufficient descent property.

1. Introduction

The CG method is a well-established class of algorithms widely used for solving large-scale optimization problems. Its popularity is mainly due to the simplicity of the iterative scheme, the fast convergence properties, and the low memory requirements. In this study, we consider the following unconstrained optimization problem:

$$\min_{x \in \mathbb{R}^n} f(x). \quad (1)$$

Let $f(x): \mathbb{R}^n \rightarrow \mathbb{R}$ denote the differentiable objective function, where $x \in \mathbb{R}^n$ represents an arbitrary n -dimensional vector. For convenience, we define $g_k = \nabla f(x_k)$ as the gradient at iteration k , and $y_k = g_{k+1} - g_k$ as the difference between successive gradients. Owing to its simple iterative structure, low memory requirements, and remarkable numerical efficiency, the CG method is considered one of the most effective algorithms for solving unconstrained optimization problems. The iterative scheme of the CG method can be formulated as:

$$x_{k+1} = x_k + \alpha_k d_k. \quad (2)$$

The positive step size α_k is determined by a line search procedure. In this paper, we employ the strong Wolfe–Powell (SWP) line search, which requires α_k to satisfy the following two inequalities:

* Corresponding Author.

¹ Department of Applied Mathematics, University of Mazandaran, Babolsar, Iran, Email: Mariyatoofan74@gmail.com.

² Research Center of Optimization and Logistic (RCOL), University of Mazandaran, Babolsar, Iran.

³ Department of Basic Sciences, Rahman Institute of Higher Education, Ramsar, Iran. Email: gshakoori2@gmail.com

$$f(x_k + \alpha_k d_k) \leq f(x_k) + \delta \alpha_k g(x_k)^T d_k, \quad (3)$$

$$|g(x_k + \alpha_k d_k)^T d_k| \leq -\sigma g(x_k)^T d_k. \quad (4)$$

Where δ and σ are positive constants such that $0 < \delta < \sigma < 1$. In formula (2), the term d_k denotes the k -th search direction, also referred to as the descent direction, which is initialized as $d_0 = -g_0$. The recursive relation is given by:

$$d_{k+1} = -g(x_{k+1}) + \beta_k d_k \quad k \geq 0 \quad (5)$$

Here, β_k represents the CG coefficient, a crucial parameter that governs the update of the search direction and significantly affects the convergence behavior of the algorithm. Different choices of β_k lead to distinct optimization strategies. Among the most widely used variants are the Fletcher–Reeves (FR) method and the Polak–Ribiere–Polyak (PRP) method:

$$\beta_K^{FR} = \frac{\|g_{k+1}\|^2}{\|g_k\|^2}, \quad \beta_K^{PRP} = \frac{g_{k+1}^T y_k}{\|g_k\|^2}.$$

These approaches play a fundamental role in optimization, as they determine how the search direction evolves across iterations and thereby influence the efficiency and robustness of the method.

Following the introduction of these classical approaches, researchers developed numerous enhanced CG methods. Among these advancements, Wei et al. [14] introduced a modified version of the PRP method, referred to as the WYL method. The corresponding formula is:

$$\beta_K^{WYL} = \frac{\|g_{k+1}\|^2 - \frac{\|g_{k+1}\|}{\|g_k\|} g_{k+1}^T g_k}{\|g_k\|^2}.$$

In comparison to the PRP method, the WYL approach incorporates an additional ratio involving the covariance coefficients and the gradient paradigms, expressed as $\frac{\|g_{k+1}\|}{\|g_k\|}$. This adjustment enhances convergence performance by enabling adaptive modifications to the step size, particularly in optimization problems that involve dimensions which vary partially. Nevertheless, refining the WYL method also escalates computational complexity, ultimately resulting in slower convergence rates. Jiang et al. [9] introduced the JPRP method, whose CG coefficient combines features of both the PRP and WYL methods, and is defined by the following formula:

$$\beta_K^{JPRP} = \frac{\|g_{k+1}\|^2 - \frac{\|g_{k+1}\|}{\|g_k\|} g_{k+1}^T g_k}{\max \{\mu |g_{k+1}^T d_k|, \|g_k\|^2\}}.$$

Under the condition that $\mu > 1$ and applying a standard Wolfe line search, the author demonstrated the global convergence of this method. Building on the inspiration from the JPRP method, Hu et al. [7] introduced the NPPR methods. These methods were designed to improve the efficiency of CG techniques by refining the updates for search directions and enhancing convergence behavior. The CG coefficient for this method is:

$$\beta_K^{NPPR} = \frac{\|g_{k+1}\|^2 - \frac{\|g_{k+1}\|}{\|g_k\|} g_{k+1}^T g_k}{\max \{\mu \|g_{k+1}\| \|d_k\|, \|g_k\|^2\}}, \quad \mu > 1.$$

Dai and Wen [3] proposed modified NPPR method as follows:

$$\beta_K^{DPRP} = \frac{\|g_{k+1}\|^2 - \frac{\|g_{k+1}\|}{\|g_k\|} |g_{k+1}^T g_k|}{\mu |g_{k+1}^T d_k| + \|g_k\|^2}, \quad \mu > 1.$$

In recent years, a variety of new CG formulas have been proposed to enhance computational efficiency and improve convergence rates. A major challenge with classical CG methods lies in their inconsistent performance: while some variants may converge slowly or even stagnate on certain unconstrained optimization problems, others achieve faster progress at the expense of overall convergence reliability. To address these issues, researchers have sought to refine CG strategies with the goal of achieving a more balanced trade-off between computational speed, convergence stability, and practical effectiveness.

In the following sections, we will review additional modifications; for example, Ibrahim and Salihu [8] introduced a new modification of the CG method, referred to as the IMRMIL method. The proposed coefficient is defined as:

$$\beta_K^{IMRMIL} = \frac{g_{k+1}^T y_k - g_{k+1}^T d_k}{\|d_k\|^2}.$$

The proposed IMRMIL coefficient fulfills both the sufficient descent condition and the convergence criterion. Consequently, the generated search directions guarantee descent without additional restrictions, and the global convergence of the algorithm is established under standard Wolfe line search assumptions.

Mrad and Fakhari [11] proposed a modified spectral CG algorithm for unconstrained optimization problems. The CG coefficient is defined as:

$$\beta_K^{MF} = \begin{cases} 0 & \frac{g_{k+1}^T d_k}{g_k^T d_k} \leq c_1 \\ \max(0, \min(\beta_K^{LS}, \beta_K^{CD})) & c_1 < \frac{g_{k+1}^T d_k}{g_k^T d_k} \\ \delta \frac{\|g_{k+1}\|^2}{g_{k+1}^T d_k} & \frac{g_{k+1}^T d_k}{d_k^T y_k} \geq c_2 \end{cases}$$

This algorithm employs Wolfe inexact line search conditions to determine the step length at each iteration and adaptively selects the appropriate CG coefficient. Numerical experiments on a variety of unconstrained functions demonstrated that the method is highly stable regardless of the starting point, and in several cases achieves faster convergence and higher efficiency compared to classical CG methods.

Building upon prior studies, this paper aims to introduce a simpler CG method that ensures the descent condition and convergence. The previous methods remain important and effective, but our approach provides a more direct formulation with clear convergence properties.

This paper presents a newly modified nonlinear CG method, developed by extending the approaches of Dai and Wen [3] and Hu et al. [7]. The proposed formula and algorithm are described in detail in Section 2. Section 3 establishes the global convergence of the method under Wolfe line search conditions, with a rigorous proof provided. Section 4 reports extensive numerical experiments, highlighting the performance of the proposed method in comparison with several classical and modern CG variants.

2. New spectral CG

Building upon the concepts introduced by the NPPR and DPRP methods, this paper proposes a novel approach, referred to as the MFR method. In this formulation, the denominator of the CG coefficient is retained from the NPPR method, while the numerator is slightly modified by incorporating elements of the Fletcher–Reeves (FR) strategy. In this way, the proposed formula integrates the strengths of both NPPR and FR approaches. The detailed expression of the MFR coefficient is given by:

$$\beta_K^{MFR} = \frac{\|g_{k+1}\|^2 - \min(\frac{|g_{k+1}^T d_k|}{\|g_{k+1}\| \|d_k\|}, \|g_{k+1}\|^2)}{\max\{\mu \|g_{k+1}\| \|d_k\|, \|g_k\|^2\}}, \mu > 2 \quad (6)$$

$$\begin{aligned} \theta &= \frac{-\|g_{k+1}\|^2}{-\|g_{k+1}\|^2 + \beta_K^{MFR} g_{k+1}^T d_k}, \\ d_{k+1} &= -\theta g_{k+1} + \theta \beta_K^{MFR} d_k. \end{aligned} \quad (7)$$

It is worth noting that the MFR method establishes a sufficient descent condition

$$g_{k+1}^T d_{k+1} = -\|g_{k+1}\|^2, \quad (8)$$

which serves as a necessary step for proving convergence, expressed in the form of an equality. Here is the detailed algorithm:

Algorithm 1: MFR Method

- Step 1: Initialize with a starting point $x_0 \in \mathbb{R}^n$, set $\epsilon > 0$ and constants $0 < \delta < \frac{1}{2}$, $\delta < \sigma < 1$. Assign initial values for variables as $d_0 = -g_0$, $k = 0$.
- Step 2: Check the stopping criterion. If $\|g_k\| < \epsilon$ terminate the algorithm. Otherwise, proceed to Step 3.
- Step 3: Compute β_K^{MFR} using Equation (6) and calculate d_k based on Equation (7).
- Step 4: Determine α_k using the SWP line search method derived from Equations (3) and (4).
- Step 5: Update the solution as $x_{k+1} = x_k + \alpha_k d_k$, then increment k by 1. Return to Step 2.

3. Global Convergence Analysis

To demonstrate the global convergence of the proposed method, this paper begins by introducing Assumption 3.1.

Assumption 3.1:

- A: The set, represented as $K = \{x \in \mathbb{R}^n; f(x) \leq f(x_0)\}$ constitutes the level set that is bounded.
- B: Within a specified neighborhood D of the set, the function K is continuously differentiable and adheres to the following inequality: $\|g(x) - g(y)\| \leq L \|x - y\|$ where $x, y \in D$ and $L > 0$.

Lemma 3.1: Given that Assumption 1 holds, consider any CG defined by equations (2) and (5), where the condition $g_{k+1}^T d_{k+1} = -\|g_{k+1}\|^2$ is satisfied. Furthermore, let α_k fulfill the SWP line search criteria specified in equations (3) and (4). As a result, the following inequality holds:

$$\sum_{k=1}^{\infty} \frac{(g_{k+1}^T d_{k+1})^2}{\|d_k\|^2} < \infty \quad (9)$$

Additionally, substituting equation (8) into inequality (9), leads to:

$$\sum_{k=1}^{\infty} \frac{\|g_{k+1}\|^4}{\|d_k\|^2} < \infty.$$

This lemma is commonly known as the Zoutendijk condition and is satisfied under the SWP line search framework, as discussed in [1].

Theorem 3.1: If Assumption 1 holds, β_k is determined by equation (6), and x_k is obtained using Algorithm 1. Moreover, α_k satisfies the SWP line search conditions outlined in equations (3) and (4), with parameters $0 < \delta < \sigma < \frac{1}{2}$, $\mu > 2$. Then:

$$\lim_{k \rightarrow \infty} \|g_k\| = 0.$$

Remark 3.1: Consider the case where we define

$$d_{k+1} = \begin{cases} d_{k+1}^{MFR} & \|d_{k+1}^{MFR}\| < M \\ -g_{k+1} & \text{otherwise} \end{cases}$$

where a restart is implemented whenever $\|d_{k+1}^{MFR}\|$ falls below a prespecified large constant M . Under this condition, it can be observed that the MFR method demonstrates convergence.

4. Numerical experiments

To evaluate the computational performance of the proposed methods, we present several numerical experiments, comparing MFR, NPRP, DPRP and FR. The implementation of all codes was carried out in MATLAB, tested on 96 functions from the CUTER [5] test suite, as listed in Tables 1-6. Comprehensive details regarding the software and hardware specifications are available in [10]. The approximate Wolfe conditions outlined in [6,14] were utilized in our implementations, maintaining the same parameter values (specifically, $\delta = 0.1$ and $\sigma = 0.9$). The algorithms were terminated based on the same criteria detailed in [2]. To evaluate the quality of the results, we relied on the performance profile described in [4], using the notation from [2]. This assessment was conducted on TNFGE (total number of function and gradient evaluations, as defined in [6,14]) and CPUT (CPU time measured in seconds). The improvement can be attributed to enforcing the sufficient descent condition in equality form, which stabilizes the search directions and accelerates convergence. These findings demonstrate that the proposed spectral modification not only ensures theoretical convergence but also delivers practical computational advantages, making it a promising alternative for large-scale unconstrained optimization problems.

Figure 1 illustrates the performance profile with respect to TNFGE across the tested CUTER functions. It can be observed that the proposed MFR method consistently outperforms NPRP, DPRP, and FR, achieving lower function and gradient evaluations in the majority of test cases. This indicates that enforcing the sufficient descent condition in equality form contributes to improved computational efficiency and stability of the algorithm. The outputs of the numerical experiments are reported in Tables 1-3, which summarize the performance of the proposed MFR method compared to NPRP, DPRP, and FR.

Figure 2 illustrates the comparative performance profiles of the tested algorithms with respect to CPU time, clearly showing that NPRP achieves the fastest execution, followed by MFR, DPRP, and FR. These trends confirm the efficiency of the proposed spectral modification relative to classical methods. The

detailed numerical outputs supporting these observations are reported in Tables 4–6, where the values of TNFGE and CPUT are presented for all CUTER test functions. The tabulated results provide further evidence of the stability and competitiveness of MFR compared to the other CG methods.

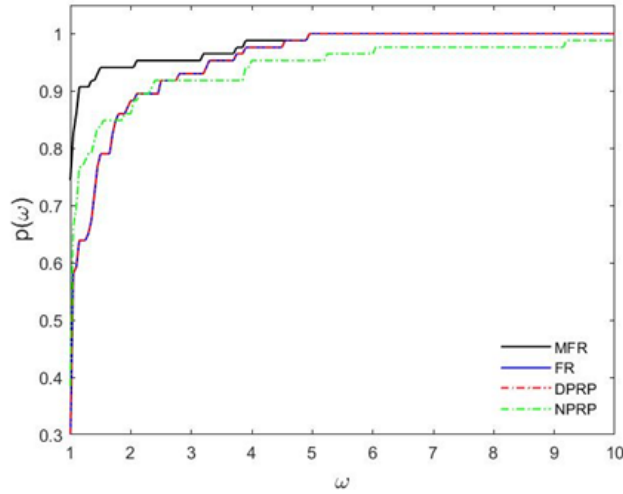


Figure 1: Outputs of comparisons by the approximate Wolfe line search with respect to TNFGE

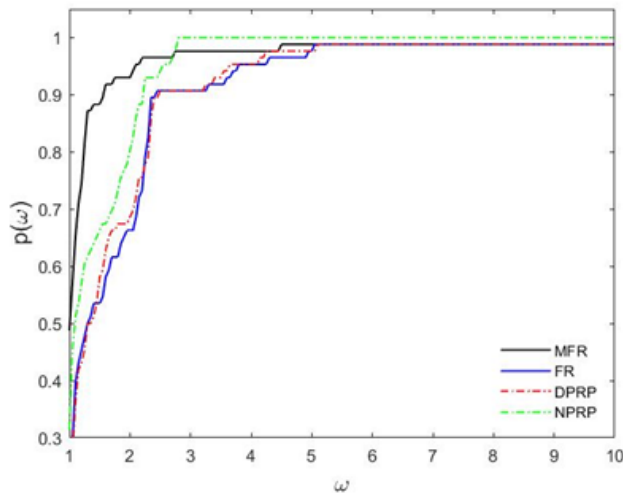


Figure 2: Outputs of comparisons by the approximate Wolfe line search with respect to CPUT

Table 1: Result based on TNFGE-Series 1

Function	Dimention	MFR	FR	DPRP	NPRP
ARGLINA	200	9	9	9	9
ARWHEAD	5000	27996	36724	36724	647
BDEXP	5000	39	49	49	29
BDQRTIC	5000	50015	50015	50015	13919
BIGGSB1	5000	69998	70041	70041	69998
BOX	10000	50004	50004	50004	4412
BQPGABIM	50	1622	2335	2335	3316
BQPGASIM	50	1622	2335	2335	3316
BQPGAUSS	2003	69998	70033	70033	69998
BRATU1D	5003	763	693	693	994
BROWNAL	200	69990	70859	70859	70030
BROYDN7D	5000	13934	14801	14801	12746
BRYBND	5000	216	411	411	513
CHAINWOO	4000	50019	54452	54452	44204
CHENHARK	5000	69998	70025	70025	69998
CHNROSNB	50	57338	50004	50004	56720
CLPLATEB	5041	50004	50015	50015	50323
COSINE	10000	123	115	115	132
CRAGGLVY	5000	1920	3339	3339	1349
CURLY10	10000	50050	50094	50094	50050
CURLY20	10000	50046	50046	50046	50046
CURLY30	10000	50042	50046	50046	50046
DECONVU	63	50004	50464	50464	50004
DIXMAANA	3000	44	49	49	403
DIXMAANB	3000	34	49	49	368
DIXMAANC	3000	44	59	59	265
DIXMAAND	3000	49	69	69	257
DIXMAANE	3000	47367	69982	69982	53801
DIXMAANF	3000	50742	69156	69156	52585
DIXMAANG	3000	50675	69228	69228	52427
DIXMAANH	3000	50465	69336	69336	53192
DIXMAANI	3000	69982	69968	69968	69958

Table 2: Result based on TNFGE-Series 2

Function	Dimention	MFR	FR	DPRP	NPRP
DIXMAANJ	3000	50004	50004	50004	50004
DIXMAANK	3000	50004	50004	50004	50822
DIXMAANL	3000	50004	50015	50015	53112
DIXON3DQ	10000	69998	70041	70041	69998
DMN15102	66	50016	50148	50148	50209
DMN15103	99	50090	50146	50146	50337
DMN37142	66	50008	50016	50016	50109
DMN37143	99	50035	50032	50032	50272
DQDRTIC	5000	5962	7999	7999	13746
DQRTIC	5000	94	104	104	363
DRCAV1LQ	4489	4	4	4	4
DRCAV2LQ	4489	4	4	4	4
DRCAV3LQ	4489	4	4	4	4
EDENSCH	2000	152	264	264	172
EG2	1000	29	29	29	29
EIGENALS	2550	50031	50410	50410	50053
EIGENBLS	2550	50004	50016	50016	50036
EIGENCLS	2652	50008	50244	50244	50105
ENGVAL1	5000	148	249	249	278
ERRINROS	50	50015	50041	50041	50081
EXTROSNB	1000	50015	50008	50008	50024
FLETCBV2	5000	50004	124408	124408	50004
FLETCBV3	5000	49	45	45	45
FLETCHBV	5000	49	49	49	45
FLETCHCR	1000	65588	65689	65689	66804
FMINSRF2	5625	50004	56504	56504	55786
FMINSURF	5625	63066	57590	57590	55242
FREUROTH	5000	16790	35051	35051	23532
GENHUMPS	5000	50047	50043	50043	50148
GENHUMPS	5000	50047	50043	50043	50148
GENROSE	500	50955	50008	50008	50012
LIARWHD	5000	50004	50011	50011	13499

Table 3: Result based on TNFGE-Series 3

Function	Dimention	MFR	FR	DPRP	NPRP
MOREBV	5000	69998	70009	70009	69998
MSQRTALS	1024	50023	50023	50023	50031
MSQRTBLS	1024	50023	50023	50023	50023
NCB20	5010	50008	51909	51909	50055
NCB20B	5000	68529	44709	44709	13872
NONCVXU2	5000	50004	50004	50004	50004
NONDIA	5000	50004	50004	50004	50311
NONDQUAR	5000	50008	50152	50152	50146
PENALTY1	1000	7775	31531	31531	2293
PENALTY2	200	9	9	9	9
PENALTY3	200	2512	2495	2495	1733
POWELSG	5000	52008	50004	50004	54854
POWER	10000	50004	50015	50015	12867
QUARTC	5000	94	104	104	363
SCHMVETT	5000	406	951	951	194
SENSORS	100	135	223	223	186
SINQUAD	5000	50045	50045	50045	34029
SPARSINE	5000	68922	68832	68832	67764
SPARSQUR	10000	134	117	117	467
SPMSRTLS	4999	19145	26518	26518	25980
SROSENBR	5000	44806	55089	55089	3139
TESTQUAD	5000	69998	71396	71396	69998
TOINTGOR	50	4021	7854	7854	4945
TOINTGSS	5000	29	95	95	29
TOINTPSP	50	4417	6274	6274	1393
TOINTQOR	50	586	1639	1639	1251
TQUARTIC	5000	50004	50030	50030	50157
TRIDIA	5000	69998	70037	70037	69998
VARDIM	200	61	79	79	69
VAREIGVL	50	214	379	379	329
WOODS	4000	28830	50004	50004	36777

Table 4: Result based on CPUT-Series 1

Function	Dimention	MFR	FR	DPRP	NPRP
ARGLINA	200	8.82E-02	1.63E-01	1.26E-01	1.48E-01
ARWHEAD	5000	4.80E+00	1.47E+01	1.48E+01	4.72E-01
BDEXP	5000	8.55E-02	1.34E-01	1.33E-01	1.20E-01
BDQRTIC	5000	1.03E+01	2.42E+01	2.44E+01	6.30E+00
BIGGSB1	5000	6.97E+00	2.48E+01	2.47E+01	1.93E+01
BOX	10000	2.27E+01	5.06E+01	5.05E+01	4.29E+00
BQPGABIM	50	9.54E-02	1.82E-01	1.20E-01	2.00E-01
BQPGASIM	50	1.13E-01	1.23E-01	1.26E-01	2.06E-01
BQPGAUSS	2003	6.76E+00	5.69E+00	6.20E+00	5.60E+00
BRATU1D	5003	7.11E+00	5.54E+00	5.51E+00	5.65E+00
BROWNAL	200	5.24E+00	1.21E+01	1.22E+01	1.17E+01
BROYDN7D	5000	9.41E+00	2.30E+01	2.31E+01	1.97E+01
BRYBND	5000	1.81E-01	4.00E-01	3.88E-01	4.53E-01
CHAINWOO	4000	8.57E+00	2.05E+01	2.09E+01	1.57E+01
CHENHARK	5000	6.41E+00	1.39E+01	1.53E+01	1.38E+01
CHNROSNB	50	2.20E+00	1.83E+00	1.81E+00	1.72E+00
CLPLATEB	5041	1.15E+01	2.60E+01	2.67E+01	2.56E+01
COSINE	10000	1.76E-01	2.74E-01	2.84E-01	2.90E-01
CRAGGLVY	5000	1.14E+00	1.73E+00	1.69E+00	7.14E-01
CURLY10	10000	1.51E+01	1.34E+01	1.34E+01	1.29E+01
CURLY20	10000	2.05E+01	1.86E+01	1.84E+01	1.87E+01
CURLY30	10000	2.69E+01	2.53E+01	2.56E+01	2.57E+01
DECONVU	63	2.21E+00	1.99E+00	1.98E+00	1.84E+00
DIXMAANA	3000	6.98E-02	8.48E-02	8.47E-02	1.92E-01
DIXMAANB	3000	6.33E-02	1.07E-01	9.24E-02	1.73E-01
DIXMAANC	3000	6.20E-02	9.40E-02	8.88E-02	1.65E-01
DIXMAAND	3000	7.25E-02	9.56E-02	1.06E-01	1.37E-01
DIXMAANE	3000	6.94E+01	1.62E+02	1.63E+02	9.00E+01
DIXMAANF	3000	3.60E+01	4.94E+01	5.37E+01	4.70E+01
DIXMAANG	3000	3.34E+01	1.65E+02	1.38E+02	3.84E+01
DIXMAANH	3000	3.66E+01	6.04E+01	6.01E+01	3.71E+01
DIXMAANI	3000	5.98E+01	5.28E+01	5.27E+01	6.41E+01

Table 5: Result based on CPUT-Series 2

Function	Dimention	MFR	FR	DPRP	NPRP
DIXMAANJ	3000	4.45E+01	5.32E+01	5.35E+01	3.92E+01
DIXMAANK	3000	4.48E+01	4.64E+01	4.64E+01	4.12E+01
DIXMAANL	3000	4.30E+01	5.41E+01	5.44E+01	4.25E+01
DIXON3DQ	10000	9.97E+00	9.46E+00	9.65E+00	9.65E+00
DMN15102	66	9.43E+01	1.95E+02	1.93E+02	1.92E+02
DMN15103	99	1.15E+02	1.14E+02	1.26E+02	1.16E+02
DMN37142	66	9.70E+01	9.52E+01	9.51E+01	9.48E+01
DMN37143	99	1.14E+02	1.13E+02	1.13E+02	1.22E+02
DQDRTIC	5000	9.28E-01	1.10E+00	1.09E+00	1.77E+00
DQRTIC	5000	8.03E-02	5.05E-02	7.38E-02	9.26E-02
DRCAV1LQ	4489	8.55E-02	8.91E-02	8.66E-02	9.64E-02
DRCAV2LQ	4489	1.05E-01	9.74E-02	8.69E-02	8.90E-02
DRCAV3LQ	4489	1.18E-01	9.66E-02	9.16E-02	1.08E-01
EDENSCH	2000	8.04E-02	9.07E-02	9.16E-02	7.50E-02
EG2	1000	7.77E-02	4.01E-02	3.74E-02	4.20E-02
EIGENALS	2550	6.67E+01	6.82E+01	6.81E+01	6.75E+01
EIGENBLS	2550	6.66E+01	6.77E+01	6.76E+01	6.74E+01
EIGENCLS	2652	7.23E+01	7.36E+01	7.36E+01	7.41E+01
ENGVAL1	5000	1.16E-01	1.37E-01	1.24E-01	1.28E-01
ERRINROS	50	2.10E+00	1.87E+00	1.83E+00	1.74E+00
EXTROSNB	1000	4.00E+00	3.21E+00	3.30E+00	3.17E+00
FLETCBV2	5000	1.82E+01	3.87E+01	3.88E+01	1.75E+01
FLETCBV3	5000	1.19E-01	1.12E-01	1.19E-01	1.17E-01
FLETCHBV	5000	1.14E-01	1.19E-01	1.10E-01	1.08E-01
FLETCHCR	1000	3.66E+00	3.34E+00	3.33E+00	3.20E+00
FMINSRF2	5625	9.41E+00	1.03E+01	1.03E+01	9.71E+00
FMINSURF	5625	1.17E+01	1.06E+01	1.08E+01	1.00E+01
FREUROTH	5000	3.96E+00	7.19E+00	7.11E+00	4.89E+00
GENHUMPS	5000	2.77E+01	2.69E+01	2.69E+01	2.83E+01
GENHUMPS	5000	2.72E+01	2.66E+01	2.61E+01	2.77E+01
GENROSE	500	2.78E+00	2.36E+00	2.38E+00	2.22E+00
LIARWHD	5000	8.48E+00	8.06E+00	7.98E+00	1.90E+00

Table 6: Result based on CPUT-Series 3

Function	Dimention	MFR	FR	DPRP	NPRP
MOREBV	5000	9.12E+00	7.43E+00	7.47E+00	7.17E+00
MSQRTALS	1024	1.48E+01	3.11E+01	3.13E+01	3.07E+01
MSQRTBLS	1024	1.50E+01	3.12E+01	3.14E+01	2.98E+01
NCB20	5010	2.64E+01	6.20E+01	6.21E+01	5.86E+01
NCB20B	5000	3.47E+01	5.17E+01	5.13E+01	1.58E+01
NONCVXU2	5000	1.73E+01	3.83E+01	3.90E+01	3.86E+01
NONDIA	5000	7.66E+00	7.33E+00	7.42E+00	7.14E+00
NONDQUAR	5000	5.71E+00	1.26E+01	1.22E+01	1.21E+01
PENALTY1	1000	5.70E-01	1.72E+00	1.66E+00	1.41E-01
PENALTY2	200	2.94E-02	2.46E-02	1.68E-02	1.08E-02
PENALTY3	200	3.36E+00	3.34E+00	3.36E+00	2.72E+00
POWELLSG	5000	5.68E+00	1.25E+01	1.25E+01	1.17E+01
POWER	10000	6.65E+01	1.13E+02	1.13E+02	4.30E+00
QUARTC	5000	1.04E-01	6.01E-02	6.73E-02	1.05E-01
SCHMVETT	5000	4.20E-01	7.78E-01	7.45E-01	2.07E-01
SENSORS	100	3.78E-01	8.05E-01	7.39E-01	6.77E-01
SINQUAD	5000	1.76E+01	4.08E+01	4.08E+01	2.67E+01
SPARSINE	5000	2.36E+01	5.51E+01	5.48E+01	5.28E+01
SPARSQUR	10000	2.10E-01	1.58E-01	1.55E-01	3.09E-01
SPMSRTLS	4999	4.33E+00	5.48E+00	5.42E+00	5.13E+00
SROSENBR	5000	4.91E+00	5.83E+00	5.82E+00	4.01E-01
TESTQUAD	5000	1.66E+01	8.36E+01	8.42E+01	2.93E+01
TOINTGOR	50	2.69E-01	6.24E-01	6.64E-01	4.04E-01
TOINTGSS	5000	8.56E-02	1.11E-01	1.12E-01	7.10E-02
TOINTPSP	50	2.05E-01	4.92E-01	4.52E-01	1.34E-01
TOINTQOR	50	3.95E-02	8.95E-02	9.19E-02	9.79E-02
TQUARTIC	5000	7.23E+00	1.53E+01	1.45E+01	1.43E+01
TRIDIA	5000	2.06E+01	4.77E+01	4.76E+01	2.56E+01
VARDIM	200	2.56E-02	2.23E-02	3.38E-02	3.01E-02
VAREIGVL	50	4.77E-02	7.26E-02	4.97E-02	3.84E-02
WOODS	4000	3.34E+00	5.53E+00	5.58E+00	3.53E+00

5. Conclusion

In this study, we introduced a spectral modification of the CG method (MFR) and demonstrated its effectiveness through extensive numerical experiments. The proposed algorithm guarantees both the sufficient descent condition and global convergence under Wolfe line search assumptions.

Numerical results on 96 CUTer test functions confirmed that MFR achieves competitive efficiency compared to NPRP, DPRP, and FR, while maintaining theoretical robustness. These findings suggest that enforcing the descent condition in equality form can provide computational advantages in large-scale unconstrained optimization. Despite these promising results, the study is limited to unconstrained optimization problems and relies on benchmark test functions, which may not fully capture the complexity of real-world applications. Future research could extend the proposed approach to constrained optimization, investigate its performance on large-scale industrial problems, and explore applications in areas such as image restoration and machine learning. These directions would further validate the practical relevance and broaden the impact of the proposed method.

References

- [1] Alhawarat, A., Salleh, Z., Mamat, M., and Rivaie, M. (2017), An efficient modified Polak–Ribi  re–Polyak conjugate gradient method with global convergence properties, *Optimization Methods and Software*, 32(6), 1299-1312.
- [2] Aminifard, Z., and Babaie–Kafaki, S., (2019), *An optimal parameter choice for the Dai–Liao family of conjugate gradient methods by avoiding a direction of the maximum magnification by the search direction matrix*, 4OR, 17:317–330.
- [3] Dai, Z., & Wen, F. (2012), Another improved Wei–Yao–Liu nonlinear conjugate gradient method with sufficient descent property, *Applied Mathematics and Computation*, 218(14), 7421-7430.
- [4] Dolan, E.D. and Mor  , J.J., (2002), *Benchmarking optimization software with performance profiles*, Math. Programming, 91(2, Ser.A):201–213.
- [5] Gould, N.I.M., Orban, D. and Toint, Ph.L. (2003) *CUTer: a constrained and unconstrained testing environment, revisited*, ACM Trans. Math. Software, 29(4):373–394.
- [6] Hager, W.W., and Zhang, H., (2006), *Algorithm 851: CG-Descent, a conjugate gradient method with guaranteed descent*, ACM Trans. Math. Software, 32(1):113–137.
- [7] Hu, O., Zhang, H., and Chen, Y., (2022), Global convergence of a descent PRP type conjugate gradient method for nonconvex optimization, *Applied Numerical Mathematics*, 173, 38-50.
- [8] Ibrahim, S. M., & Salihu, N. (2025), Two sufficient descent spectral conjugate gradient algorithms for unconstrained optimization with application, *Optimization and Engineering*, 26(1), 655-679.
- [9] Jiang, X. Z., Jin Bao, J. I. A. N., and Dong, G., (2014), Two Conjugate Gradient Methods with Sufficient Descent Property, *Acta Mathematica Sinica, Chinese Series*, 57(2), 365-372.
- [10] Mirhoseini, N., Babaie–Kafaki, S., and Aminifard, Z., (2022), A nonmonotone scaled Fletcher–Reeves conjugate gradient method with application in image reconstruction, *Bull. Malays. Math. Sci. Soc.*, 45:2885–2904.
- [11] Mrad, H., & Fakhari, S. M. (2024), Optimization of unconstrained problems using a developed algorithm of spectral conjugate gradient method calculation, *Mathematics and Computers in Simulation*, 215, 282-290.
- [12] Ranjbar, M., & Ashrafi, A. (2025). A modified hybrid three-term conjugate gradient method and its applications in image restoration. *Iranian Journal of Operations Research*, 16(1), 1-17.
- [13] Toofan, M., & Babaie–Kafaki, S. (2026). Hybrid Conjugate Gradient Methods Based on an Extended Least-Squares Model: M. Toofan, S. Babaie–Kafaki. *Vietnam Journal of Mathematics*, 54(1), 205-213.
- [14] Wei, Z., Yao, S., and Liu, L., (2006), The convergence properties of some new conjugate gradient methods, *Applied Mathematics and Computation* 183(2), 150.